

Modeling quantitative interactions: the disease outcome of generalist fungal pathogen across the plant kingdom

Celine Caseys¹, Gongjun Shi², Nicole Soltis³, Raoni Gwinner⁴, Jason Corwin⁵, Susanna Atwell³, and Daniel Kliebenstein³

¹University of California Davis

²North Dakota State University

³UC Davis

⁴Embrapa Amazonia ocidental, Manaus

⁵University of Colorado at Boulder

November 14, 2020

Abstract

Botrytis cinerea is a fungal pathogen that causes necrotic disease on more than a thousand known hosts widely spread across the plant kingdom. How *B. cinerea* interacts with such extensive host diversity remains largely unknown. To address this question, we generated an infectivity matrix of 98 strains of *B. cinerea* on 90 genotypes representing eight host plants. This experimental infectivity matrix revealed that the disease outcome is largely explained by variations in either the host resistance or pathogen virulence. However, the specific interactions between host and pathogen account for 16% of the disease outcome. Furthermore, the disease outcomes cluster among genotypes of a species but are independent of the relatedness between hosts. When analyzing the host specificity and virulence of *B. cinerea*, generalist strains are predominant. In this fungal necrotroph, specialization may happen by a loss in virulence on most hosts rather than an increase of virulence on a specific host. To uncover the genetic architecture of *Botrytis*, a genome-wide association study (GWAS) was performed and revealed 124 genes associated with host specificity and virulence. The genetic architecture of these traits is distinct, polygenic and widespread across *B. cinerea* genome. The complexity of the disease outcome is best explained by the additivity of small effect genes that adjust the infection to diverse hosts.

Introduction

Plants and their pathogens exist within ecosystems that create diverse combinatorial abiotic and biotic pressures (Glazebrook & Roby 2018). The additivity of these various pressures opens the question of how does it translate into the genome of species and impact specific interactions to ecosystems? Answering this question remains a challenge, especially given the diversity of interactions, ranging from within (e.g. plant-plant) to across kingdom (e.g. plant-pathogen) interactions and from mutualism to predation. When focusing on plant-pathogen interactions, various levels of complexity are found in nature. Historically, the predominant focus of research has been on pairwise interactions (e.g. one plant, one pathogen) but more complex plant-pathogen network wherein a plant or pathogen interacts with a broader range of organisms is now trending (Delplace *et al.* 2020; Zhang *et al.* 2019).

The range of plant-pathogen interactions has created a myriad of pathogen virulence mechanisms (mechanisms with detrimental effects to a host) to attack and/or interfere with the plant resistance (the hosts capacity to fight the pathogen back;(Lannou 2012)). Virulence mechanisms vary across the continuum of pathogens lifestyles and host specificity (Barrett *et al.* 2009; Cowger & Brown 2019; Frantzeskakis *et al.* 2020). At one end of the continuum, specialist biotrophs develop intricate relationships, living and feeding

within the host tissues. At the other end, generalist necrotrophs attack, kill and feed on degraded tissues. The pressure on pathogens to specialize also varies across the continuum of lifestyles. Some pathogens develop specific and intricate responses to their host (e.g. biotrophs), while other pathogen interactions are broad ranging (e.g. saprophytes) (Krah *et al.* 2018; Leggett *et al.* 2013). Pathogens also cover a large range from specialists attacking one or few hosts to generalists that can have multiple hosts, taxonomically related or not. Both the lifestyle and host-specificity can influence the genetic architecture of the plant-pathogen interaction (Barrett *et al.* 2009; Morris & Moury 2019). This leads to diverse genetic architectures that can explain the specificity and virulence of pathogens (Möller & Stukenbrock 2017; Morris & Moury 2019). In pathosystems following the co-evolution model such as *Magnaporthe oryzae* and *Phytophthora infestans*, few avirulence factors in the pathogen and resistance proteins in the host dictate the interactions (Bialas *et al.* 2018; Brown & Tellier 2011; Upson *et al.* 2018). Pathogens such as *Fusarium oxysporum* and *Alternaria alternata* comprise individual strains that display host specialization linked to accessory chromosomes (Bertazzoni *et al.* 2018; Plissonneau *et al.* 2017; van der Does & Rep 2007). Other fungal plant pathogens such as *Ustilago maydis* have compartmentalized genomic regions with rapidly evolving gene clusters (Möller & Stukenbrock 2017; Plissonneau *et al.* 2017). Large-effect genes dominate such qualitative genetic architecture with two-speed genome architectures being frequent (Dong *et al.* 2015; Plissonneau *et al.* 2017). Finally, pathogens such as *Sclerotinia sclerotiorum* and *Microbotryum lychnidis-dioicae* rely on quantitative genetic architectures based on hundreds of small effect loci (Corwin & Kliebenstein 2017; Cowger & Brown 2019; Lannou 2012; Poland *et al.* 2009). As advanced models of quantitative architectures, recent transcriptomic studies show that necrotrophs have intricate interactions with hosts by altering gene networks involved in signaling, regulation of cellular processes, transport, metabolism and proteolysis (Delplace *et al.* 2020; Zhang *et al.* 2019).

As a host, a plant can be exposed to multiple pathogens with various attack strategies. As counter-measures to the diversity of pathogens, plants have developed multi-layered resistance mechanisms ranging from constitutive physical defenses to inducible responses coordinated by the plant immune system upon the recognition of danger (Glazebrook 2005; Herman & Williams 2012; Wilkinson *et al.* 2019). The individual components in these multi-layered defense systems have complex and diverse evolutionary histories. Defense components such as resistance genes (Jacob *et al.* 2013) or specialized defense compounds (Chae *et al.* 2014) are frequently specific to limited lineages or even individual plant species. In contrast, other components such as the cell wall (Sorensen *et al.* 2010), defense hormone signaling (Berens *et al.* 2017) or reactive oxygen species (Inupakutika *et al.* 2016) are widely shared across plant lineages. Crop domestication further complicates the pattern of plant resistance through artificial selection. Crop domestication can create a loss of genetic diversity and canonical reductions in plant defense compounds (Chen *et al.* 2015; De Gracia *et al.* 2015; Karasov *et al.* 2014; Whitehead *et al.* 2017). It remains to clarify how these various evolutionary histories of plant resistance contribute to the plant-pathogen interactions.

In this study, we use the necrotrophic fungus, *Botrytis cinerea* (grey mold) to estimate the relative contribution of variation across multiple hosts in shaping the host-strain interactions. *Botrytis cinerea* causes billions/annum of crop damage both pre- and post-harvest to various crops from ornamentals to vegetables and fruits (Fillinger & Elad 2015; Veloso & van Kan 2018). It has a broad host range ranging from mosses to gymnosperms to eudicots, and is classically considered as a generalist fungal pathogen. An analysis of known (Elad *et al.* 2016) hosts showed that the eudicots contains 71% of the plant species with documented *Botrytis* disease symptoms, currently 996 species widely spread across orders (Fig.1). *Botrytis cinerea* has extensive standing genetic variation in both local and global populations (Atwell *et al.* 2018; Atwell *et al.* 2015; Bardin 2018; Calpaset *et al.* 2006; Ma & Michailides 2005; Walker *et al.* 2014). In addition, *B. cinerea* spores are widespread within the environment ranging from presence on plants to presence on non-plant substrates including within rain, indicating an ability to spread rapidly and widely (Bardin 2018; Leyronas *et al.* 2015). In the *Botrytis*-*Arabidopsis* pathosystem, genome-wide association studies (GWAS) detected complex genetic architectures in both *A. thaliana* and *B. cinerea*. In *Arabidopsis*, resistance genes accounted only a small proportion of candidate genes that were connected to disease resistance, signaling, reactive oxygen species and other developmental processes such as light signal transduction (Corwin *et al.* 2016; Fordyce *et al.* 2016).

al. 2018). In *B. cinerea*, genes part of networks associated with vesicular transport, degradation enzymes, metabolism and cellular processes are frequently identified (Soltis *et al.* 2019; Soltis *et al.* 2020; Zhang *et al.* 2019).

Because *B. cinerea* strains infect a large array of species (Fig. 1), it is possible to empirically assess how host resistance and strain virulence contribute to the disease outcome. We generated infectivity matrices for 90 plant genotypes from eight eudicot species against 98 diverse *B. cinerea* strains under experimental conditions in a standardized environment to ask a set of questions about this generalist pathogen. First, how do genetic diversity among and within eight hosts and among *Botrytis*' strains contribute to the disease outcome? Second, do crop domestication and phylogenetic distances consistently influence the interactions with this generalist pathogen? And finally, how do the genomic architecture of virulence and host specificity relate within this generalist pathogen?

Material & Methods

Plant material and growth condition

The experimental design of this study (Fig. S1) was chosen to assess the effect of genetic diversity in and between crops in interaction with *Botrytis cinerea*. It considers four Asterales, one Solanales, one Fabales, and two Brassicales, covering various phylogenetic distances, centered on the Asterales, a family with large species diversity and frequently hosting *B. cinerea* (Fig.1). While the chosen species partially represent the eudicot phylogeny, they were also chosen to represent the diversity of plant domestication syndromes and geographical origins (Meyer *et al.* 2012) (Fig. S2). *Helianthus annuus* and *Glycine max* were domesticated for seeds, *Solanum* for fruit (Lin *et al.* 2014) while *Lactuca*, *Cichorium intybus* and *Cichorium endivia* were domesticated for leaf and root (Dempewolf *et al.* 2008). All of these species underwent a single domestication event while *Brassica rapa* domestication is more complex being domesticated multiple times for multiple traits including seed, leaf and root characteristics (Bird *et al.* 2017).

Within each plant species, six genotypes were chosen to represent the genetic diversity in the high improvement germplasm (cultivar, inbred lines) while six genotypes represented the low improvement germplasm (wild, landraces) (Fig.S1). The genotypes were chosen within the seed collections of the US department of agriculture, the UC Davis Tomato Genetics Resource Center and the Center for Genetic Resources Netherland (CGN), with the help of experts on these collections to maximize genetic diversity, as known in 2014 at the beginning of this project. For simplicity in the language, we refer to the different crops as 'species' although referring to taxa would be more appropriate for tomato and lettuce for which we selected sister species for wild and domesticated genotypes. When referring to *Lactuca* (lettuce), *Lactuca sativa* was sampled for domesticated varieties and *Lactuca serriola* for wild accessions (Walley *et al.* 2017). When referring to *Solanum* (tomato), *Solanum lycopersicum* was sampled for domesticated varieties and *Solanum pimpinellifolium* for wild accessions native from Ecuador and Peru (Lin *et al.* 2014). Landrace genotypes were selected for *C. endivia* for which no wild relative is known and two genotypes of *B. rapa* (Fig. S2, S1). For soybean the comparison was within *G. max* as the growth behavior, vining, and growth conditions, tropical, for wild soybean, *G. soja*, was sufficiently different as to unnecessarily confound the comparison. While none of the crop species have been explicitly bred for resistance to *B. cinerea*, domestication of lettuce and chicory did shift their growing conditions towards leaves densely compacted and adaptation to colder and wetter environments, two traits associated with increased *B. cinerea* prevalence (De Vries 1997; Dempewolf *et al.* 2008; Mou 2011). Domestication in all of these species has also been associated with significant changes in their interactions with insects and specialist pathogens (Chen *et al.* 2015; De Gracia *et al.* 2015; Karasov *et al.* 2014; Whitehead *et al.* 2017).

Arabidopsis thaliana was used as a reference for genotypes with single gene alterations in major plant defense. This reference dataset is composed of Col-0 and five knockout mutants altering plant immunity (Atwell *et al.* 2018; Zhang *et al.* 2017), through the jasmonic pathway (*anac055*, *coi1*), salicylic pathway (*npr1*, *tga3*) and camalexin pathway (*pad3*), an anti-fungal defense compound in *Arabidopsis*.

Cichorium endivia, *C. intybus*, *B. rapa*, *G. max* and *A. thaliana* seeds were directly sowed in standard

potting soil. *Solanum* and *Lactuca* seeds were bleach-sterilized and germinated on wet paper in the growth chamber using flats covered with humidity domes. After 7 days, the seedlings were transferred to soil. Seed surface sterilization and scarification was used for *H. annuus* to increase seed germination. Seeds were surface sterilized in 30% bleach for 12 minutes, followed by rinsing with sterilized distilled water, and then soaked in sterilized water for 3 hrs. 1/4 of the seeds were cut off from the cotyledon end, then placed in 100 mg/L gibberellic acid for 1 hour, followed by rinsing several times with sterilized distilled water. Treated seeds were then put in covered sterilized Petri dishes with wet sterilized germination disks at 4degC for 2 weeks and sowed.

All plants were grown in growth chambers in pots containing Sunshine Mix#1 (Sun gro Horticulture, Agawam, MA) horticulture soil at 20degC with 16h hours photoperiod at 100-120 mE light intensity. All plants were watered every two days with deionized water for the first two weeks and then with nutrient solution (0.5% N-P-K fertilizer in a 2-1-2 ratio; Grow More 4-18-38). All infection experiments were conducted on mature (non-juvenile) fully developed leaves collected on adult plants that grew in these conditions for four to eight weeks (Table S2) to account for the different developmental rates. As it is challenging to fully compare developmental stages across species (soybean stages are defined by nodes, sunflower by leaf size and so on), all leaves for the assays were collected on plants in the vegetative phase at least several weeks before bolting initiation to minimize ontogenetic effects.

Botrytis collection

This study is based on a collection of 98 strains of *Botrytis cinerea* that samples fourteen plant hosts and to a smaller degree geographical origins. Ninety percent of the strains were isolated in California, largely in vineyards on UC Davis campus, while the remaining 10% of the collection are worldwide strains (Table S3). The spore collection is maintained for long-term preservation as conidial suspension in 60% glycerol at -80degC. The strains were grown for each experiment from spores on peach at 21degC for two weeks.

All strains were previously whole-genome sequenced (WGS) to an average 164-fold coverage (Atwell et al., 2018). All reads were aligned to B05.10 genome assembly ASM83294v1 (Van Kan et al. 2017) and subsequent analyses were done with 271,749 SNPs at MAF 0.20 and less than 20% of missing calls (Soltis et al. 2019). These thresholds were chosen due to the high genetic diversity detected (on average a genetic variant every 27bp, (Atwell et al. 2018)) and the potential role of structural variations in generating missing data.

In California, no evidence of host-specialization or local population structure has previously been found (Cosseboom et al. 2019; Ma & Michailides 2005; Saito & Xiao 2018; Soltis et al. 2019). To further confirm absence of population structure in the collection that also include the worldwide samples, we estimated the strain relatedness and calculated the genetic differentiation (Fst) between Californian and worldwide strains. The SNP table was converted into phylip format using PGD-spider (Lischer & Excoffier 2011) and plotted in Splitstree (Huson & Bryant 2006). For Fst estimation, the vcf file was imported with the R package vcfr and converted to the genind format. The Fst values were calculated using all SNPs with the hierfstat package (Goudet 2005) following (Weir & Cockerham 1984).

Detached leaf assay

To maximize the comparability across the diverse collection of wild relatives and crop species domesticated for different trait, leaves were chosen as a common plant organ. Detached leaf assays were conducted on adult leaves (Corwin et al. 2016; Denby et al. 2004). In brief, leaves were cut and added to trays filled with 1cm of 1% phyto-agar. The phyto-agar provided water and nutrients to the leaf that maintained physiological functions during the course of the experiment. Botrytis spores were extracted in sterile water, counted with a hemacytometer and sequentially diluted with 50% grape juice to 10 spores/ul. Drops of 4ul (40 spores of Botrytis) were used to inoculate the leaves. From spore collection to inoculation, Botrytis spores were maintained on ice to stop spore germination. Spores were maintained under agitation while inoculating leaves to keep the spore density homogeneous and decrease technical error. The inoculated leaves were maintained under humidity domes under constant light. For each host tested, the experiment included three replicates for each strain x plant genotype in a randomized complete block design and were repeated over

two experiments for a total of six replicates per strain x plant genotype.

The lesion area is a quantitative measurement of the interaction between the fungus and the host plant. To render a project of this size possible, a single time point was chosen to measure the plant-Botrytis interaction. At 72 hours post infection (hpi), the lesions are well defined on all targeted species but have not reached the edges of the leaves and thus are not tissue limited. Spore germination assays in 50% grape juice showed that strains germinate within the first 12 hours. On all species, the same pattern of growth was observed: after 48h most strains are visible within the leaf with the beginning of lesion formation. From 36h onward, Botrytis growth is largely linear and grows until the entire leaf is consumed (Rowe *et al.* 2010).

Image analysis

Each experimental tray, an unit of the randomized complete block design, was photographed in full at a fixed distance using a camera stand and an 18 Mp T3i Canon camera outfitted with an EF-S 10-22mm f/3.5-4.5 USM ultra-wide angle lens. Two lateral lamps and a white background reflecting light were used to minimize shading. The images were saved in jpeg format and analyzed with an R pipeline (Fordyce *et al.* 2018). In short, the images were transformed into hue/saturation/value (hsv) color space and threshold accounting for leaves color and intensities were defined for each species. Masks marking the leaves and lesions were created by the script and further confirmed manually. The lesions were measured by counting the number of pixels of the original pictures within the area covered by the lesion mask. The numbers of pixels were converted into centimeter using a reference scale within each image.

Data quality control

A dataset of 51,920 lesions was generated in this project but not all leaves inoculated with Botrytis developed a visible lesion at 72hpi. These ‘failed lesions’ can be explained either by technical or biological failures. Technical failures, such as failed spore germination, stochastic noise or other non-virulence related issues can bias the true estimates of the mean. To partition biological from technical failures, the lesion area distribution was analyzed for each species and thresholds were fixed as the top of the first bell curve (Table S4). These small areas are either small lesions or the spread of the inoculation drop without lesions, considered as a technical error. Therefore, a lesion below that size threshold was considered a technical error only if the median of lesion area for a plant genotype - strain pair was larger than the threshold. The rationale is the following: when most lesions within a host-Botrytis comparison are of small size, the likelihood of biological reasons for such small lesion areas is high. In contrast when the majority of lesion areas in a host-Botrytis comparison are large, it is likely that any outlier small lesions are due to technical errors like pipetting issues is high. A total of 6,395 lesions (13% of all lesions) were considered as technical failures and removed from the dataset. All statistical analyses and modeling were run on both original and filtered datasets. The removal of technical failures does not impact the effect size of the estimates but simply allowed for more variance to be attributed to biological terms in the model and less in the random error term. This is as expected when partitioning out predominantly technical failures.

Statistical analysis

All data handling and statistical analyses were conducted in R. Lesion area was modeled independently for each species using linear mixed models with the lme4 package. Variance estimates were converted into percentage of total variance to ease the comparison of the different models.

To test the respective contribution of host resistance and pathogen virulence into the disease outcome for each host species individually, we modeled the lesion area according to the host (PlantGeno) and pathogen (Strain) genotypic interactions while correcting for experimental error. The plant genotypes were nested within their improvement status (high or low) for each species.

Linear mixed model: $\text{Lesion.Area} \sim \text{Strain} + \text{Improv} + \text{Improv/PlantGeno} + \text{Strain*Improv} + \text{Strain*Improv/PlantGeno} + (1|\text{Exp.Replicate}) + (1|\text{Exp.Tray}) + (1|\text{Indiv.Plants})$

Experimental replicate (experiment 1 or 2) and trays (micro-environment with a subset of infected leaves

within the randomized complete block design) as well as the individuals plants on which were collected the leaves for the detached leaf assay are considered as random factors. Plant genotypes and *Botrytis* strains were coded as fixed factors, although they represent random sampling of the plant and fungal species. This simplification of the model was done because previous research (Corwin *et al.* 2016; Fordyce *et al.* 2018) showed that this does not influence the effect size or significance of the estimates, and dramatically decreases the computational requirements to run the model.

To incorporate the data across the host species and test the respective contributions of the host diversity, crop domestication and pathogen virulence into the disease outcome, a meta-analysis linear model was run. The improvement status or plant genotypes were nested within the plant species to account for their common evolutionary history and possibly shared resistance traits of genotypes associated with the domestication bottleneck.

Linear model: $\text{Mean.Lesion.Area} \sim \text{Strain} + \text{Species} + \text{Species/Improv} + \text{Species/PlantGeno} + \text{Strain*Species} + \text{Strain*Species/Improv}$

This modeling was performed on the mean lesion area of replicates rather than individual lesions. Given that the experimental design allows controlling for three random factors, model corrected least-square mean (LS-mean) of each genotype infected with each strain were calculated with the emmeans function using the Satterwaite approximation (Lenth *et al.* 2018).

To visualize the disease outcome resulting of the individual interactions of the 91 *Botrytis* strains and with the 90 plant genotypes (including *Arabidopsis*), a clustered heatmap was constructed on standardized LS-means with *iheatmapr* (Schep & Kummerfeld 2017). Seven isolates did not grow or sporulate in time for some of the detached leaf assays. It resulted in missing data for some of the eight species tested. These isolates were dropped for the following analyses, following concerns about the sensitivity of hierarchical clustering to missing data. The LS-means were standardized (z-score) over each plant genotypes by centering the mean to zero and fixing the standard deviation to one to overcome the large variation on lesion area across species and large variation in variance linked to the lesion area. Species with low lesion area had also small variance while species with large lesion area presented large variance. The unsupervised hierarchical clustering was run with the ‘complete’ agglomerative algorithm on Euclidean distances. The significance of the dendrogram was estimated with *pvcust* (Suzuki & Shimodaira 2006) over 20000 bootstraps. The significance of branches was fixed at $\alpha = 0.95$. For the plant genotypes dendrogram, branches were consistently assigned across hierarchical clustering methods (both ‘complete’ and ‘average’ algorithms were ran) and bootstrapping while in the *Botrytis* strains dendrogram, none of branches showed consistency.

Using our large infectivity matrix, we estimated the host specificity and overall virulence of the *B. cinerea* strains in our collection. The global virulence of each strain was calculated as the mean lesion area across the eight eudicot species. Host specificity is usually calculated qualitatively based on the broadness of presence/absence of symptoms on hosts. As *B. cinerea* is a necrotroph with quantitative disease symptoms, we estimated host specificity as the variation in disease symptom across hosts. With such estimates, generalist strains will tend to have equal virulence on various host, while more specialized strains will have increased virulence on a host relative to the other hosts. To account for variations in resistance among hosts, we used the coefficient of variation (standard deviation corrected by the mean σ/μ) of least-square mean of lesion area across the eight eudicot species (Poisot *et al.* 2012). Low host specificity indicates that strains grew consistently across the eight species, while high host specificity indicates large variation in lesion area across species, therefore higher virulence on some species.

Genome-wide association study

To estimate the respective genetic architectures of the virulence and host specificity of the strains in our collection, we performed a GWAS. Given that quantitative traits were mapped and that many statistical models work best with qualitative traits, the GWAS was performed using three different statistical models. The first model was a generalized ridge regression method for high-dimensional genomic data in *bigRR* (Shenet *et al.* 2013). This method, which tests all polymorphisms within a single model, was shown to be

adapted to estimate small effect sizes, frequent in quantitative genetic architectures. Due to the modeling of polymorphism as random factors, it estimates effect size rather than p-values. Significance of the effect size was estimated based on 1000 permutations. The 99.9% threshold was used as a conservative threshold for SNP selection. Candidate genes identified with the ridge regression approach were previously functionally validated in the *Botrytis-Arabidopsis* pathosystem (Corwin *et al.* 2016; Fordyce *et al.* 2018). The second model was a univariate linear model implemented in GEMMA (Zhou *et al.* 2013), which implement both effect size and p-values (Wald test). P-values were corrected for multiple testing based on a Bonferroni approach accounting for the genetic association of SNPs. Instead of correcting on the number of SNPs in the dataset, we used the genetic type I error calculator estimate the effective number of SNPs that account for linkage disequilibrium (Liet *et al.* 2012). The third model was a Bayesian sparse linear mixed model (BSLMM) using Markow chain Monte Carlo algorithm implemented in GEMMA (Zhou *et al.* 2013). The BSLMM model conducts the marker association tests while accounting for population structure and implementing a polygenic approach. The output of the BSLMM include estimates of the effect size and the significance, calculated as the posterior inclusion probability (PIP). The standardized relatedness matrix was calculated in GEMMA based on SNP data in the binary ped format. For each trait, 20 separate runs with 500000 burn-in and 5000000 iterations with recording every 10 steps were performed. We restricted the priors used to estimate the PVE to $0.1 < h < 0.9$ to increase convergence. For each SNP, the median of the PIP distribution of the 20 runs was used for subsequent analyses. To estimate the null distribution of the PIP, we permormed 10 random permutations of both host specificity and virulence. PIP larger than $8.2e-05$ (equivalent to 1% chance of false positive above this threshold) was considered significant based on the null distribution from the 20 randomizations. For comparison of the different three statistical models while accounting for linkage disequilibrium, we extracted the effect size estimates and calculated sliding windows with a window size of 25Kb and 10Kb steps.

For the identification of candidate genes, the significant SNPs were filtered based on two sequential criteria. First, SNPs had to be significantly associated to at least two of three GWAS methods. Secondly, we filtered the SNPs based on their potential effect. SNPs were annotated based on their location in the B05.10 genome ASM83294v1 assembly (Van Kan *et al.* 2017) with SnpEff (Cingolani *et al.* 2012). Only SNPs annotated as missense variants (modification of the amino acid in the coding region) by SnpEff and having higher probability of functional effect than up/downstream gene variants are discussed. The gene functional annotations were extracted from the fungal genomic resources portal (fungidb.org). Gene ontology and metabolic enrichment were also implemented on the online portal, however none of the enrichment analyses were significant after correction for multiple testing.

Results

Population structure in the strain collection

Although genetic differentiation follows trends of isolation by distance for most species, we observed that our strain collection contains no significant genetic stratification by either geographic or host species origin based on genome-wide SNPs (Fig.2). If genetic differentiation were structuring our strain collection, the worldwide strains would be on different branches than the *B. cinerea* strains collected in California's vineyard. Similarly, if strains had adapted specifically to growth on grapes, there would be stratification between the grape and non-grape isolates. This is confirmed by low F_{st} values between strains isolated in Europe and California with $F_{st}=0.03$ and between grape and other hosts averaging at $F_{st}=0.02$ (F_{st} range: 0 - 0.13). Because the isolates behave genomically as a single large population, we combined all the isolates to maximize statistical power in the ensuing analysis.

*Parsing the Effects of Host Resistance and *B. cinerea* Virulence*

All 90 plant genotypes were infected with 98 *B. cinerea* strains (Fig. S1) resulting in an infectivity matrix containing 51,920 independent lesion measurements. Mean lesion areas ranged from no visible damage to over 4cm^2 of necrotic leaf tissue after 72 hours of infection (Fig. 3). *Arabidopsis thaliana* has the lowest susceptibility while *H. annuus* is the most susceptible species (Fig. 3). To answer how much of the disease

outcome is explained by genetic diversity in the host and in the pathogen, we modeled the lesion area both within individual species and at large scale, as a meta-analysis across species. This approach revealed that within hosts, *B. cinerea* genetic diversity matters more than the variation in host resistance. Indeed, the effects of the genetic diversity among *B. cinerea* strains explain 40-71% of the variance in the lesion area while the pathogen interaction with the host genotypes explains 15-35% of the variance (Fig. 4B, Fig. S3B, Table S5). In contrast, the genetic variation within the plant genotypes explains between 2.8 -8-8% of the variance in the lesion area (Fig. 4B).

However, when looking at the disease outcome across the phylogeny, the resistance of the various hosts matters the most. The multi-host analysis showed that differences in host resistance between plant species account for 52% of the total variance in lesion area ($P < 2.2 \times 10^{-16}$; Fig. 4A, Table S5). Further, the interaction between the host species and *B. cinerea* strains (16% of total variance; $P < 2.2 \times 10^{-16}$) matters more than the *B. cinerea* strains alone (12% of total variance; $P < 2.2 \times 10^{-16}$). Finally, the host of origin for each strain (1.7% of total variance; $p < 2.2 \times 10^{-16}$) and the geographical origin (0.2% of total variance; $p = 0.0015$) have small effects on the lesion area, confirming the minimal influence of population structure observed at the genetic level (Fig. 2).

Botrytis cinerea and crop domestication

When infected with *B. cinerea*, tomato and lettuce wild accessions were more resistant than the domesticated ones (Fig. 3). The trend was reversed in the other five species (sunflower, endive, chicory, *Brassica* and soybean), with wild or landrace (low improvement) genotypes being less resistant than cultivars or inbred lines (high improvement, Fig. 3). While the effect of crop improvement on lesion area is statistically significant ($P < 2.2 \times 10^{-16}$), this effect is exceedingly small, 0.6% of the total variance across all plant species and 2-4% of variance within specific species models (Fig. 4, Table S5). The bi-directional small effect of domestication on this generalist pathogen is potentially an indirect effect of other selective pressures in domestication and illustrates the challenge of predicting resistance to a generalist pathogen.

Botrytis cinerea and the Eudicots

Unsupervised clustering showed that variation in host-*Botrytis* interactions identifies genotype groupings for all species, i.e. the virulence of the strains across the host genotypes is most similar within a host species. However, beyond the individual species level, the evolutionary relatedness between host species did not correlate with the similarity between the measured host-pathogen interactions (Fig. 5). For example, phylogenetically distant crops such as *B. rapa* and *Lactuca* have a similar susceptibility pattern to the 98 *B. cinerea* strains. In contrast, the two sister species, *C. endivia* and *C. intybus*, have highly divergent susceptibility patterns.

To provide a mechanistic benchmark for how the host-pathogen relationships within crops compare to single gene alterations in plant resistance, we included data for *Arabidopsis thaliana* Col-0 and five single gene knockout mutants (*coi1*, *anac055*, *npr1*, *tga3*, *pad3*). These single gene mutants have a larger effect on plant susceptibility (39% of the variance in lesion area; Fig. S3, Table S5) in comparison to variation between crop genotypes (4-8.8% of the variance within a species; Fig. 4B). While these mutants abolish major sectors of plant resistance, the *Botrytis*-host interactions still cluster these mutants to wild-type *Arabidopsis* (Fig. 5) with branch lengths comparable to variation between genotypes within crop species. Altogether, this infectivity matrix shows that the interaction of *B. cinerea* with host plants is predominantly defined by variation at a species level with little comparability between species of a particular family or genus.

Host Specificity versus Virulence

The *B. cinerea* strains cover a range of host specificity and virulence, from moderate host specificity with high virulence, to high host specificity strains with low virulence (Fig. 6). In *B. cinerea*, virulence and host specificity are not independent and best explained by a quadratic relation. The six strains that are outliers for high host specificity are also outliers for low virulence (Fig. 6A). This is illustrated by Davis Navel, a strain collected on orange that has low virulence on six hosts, moderate virulence on *Solanum sp.* (tomato) and

high virulence on *C. endivia* (Fig 6B). B05.10, the reference strain for the *B. cinerea* genome and the strain used in >90% of all papers to assess host susceptibility, is the strain with the lowest host-specificity/highest generalist behavior (Fig. 6). The B05.10 strain infects all hosts with constant and average virulence. Finally, the strains with the highest virulence have average host specificity (Fig. 6A). Katie Tomato, a strain collected on tomato that develops large lesions on all hosts is an example of high virulence strain (Fig 6B). To check whether these trends were an artifact due to a potential relation between standard deviation and mean of lesion area on which the calculation of virulence and host specificity are based, we investigated host specificity as the lesion area of each strains optimal host versus the strains average lesion area on the other 7 hosts (Fig. S4). Each strains deviation from theoretical generalism (equal virulence on all hosts, Fig. S4B) revealed a quadratic relation matching the relation between coefficient of variation based on host specificity and virulence (Fig. 6). Both metrics revealed that strains with increased host-specificity were rare in the strain collection. In combination, this suggests that *B. cinerea* is under pressure to maintain broad host ranges and moderate virulence within individual strains.

The genetic architecture of virulence and host specificity

GWAS conducted with three statistical methods (ridge regression, linear model and Bayesian sparse linear mixed models) revealed that both virulence across eight eudicots and host specificity are quantitative traits. Significantly associated SNPs are spread across 16 of the 18 chromosomes (Fig. 7, Fig. S5, Table S6). When looking at the cumulative effect of SNPs per windows along chromosomes, the quantitative architecture emerge, with numerous peaks with small to moderate effects (Fig. S5). None of the SNPs on chromosome 17 and 18, hypothesized to be potential accessory chromosomes were associated with virulence or host specificity in this dataset (Fig. 7, Table S6). The spread of significant SNPs across 16 chromosomes and regions (Table S6) observed with all three GWAS methods suggests that the genetic architecture of virulence and host specificity does not target specific genomic areas.

Filtering for SNPs based on significance in at least two GWAS approaches and annotation as missense variants revealed 73 genes associated with virulence and 51 genes associated with host specificity (Table S7). The genetic architecture of virulence and host specificity is different as only six genes are associated to both traits (Fig 7, Table S7). Among those six genes, Bcin11g05830 is a ferroportin with iron transmembrane transporter activity while Bcin07g05630 and Bcin08g05360 are transcription factors with Zn2/Cys6 DNA-binding domain. The three other genes have unknown functions. Candidate genes for virulence include a polygalacturonase known to modulate virulence (BcPG1, Bcin14g00850), a cellulase catalyzing the decomposition of cellulose (Bcin05g03390), two ABC transporters (Bcin02g06110, Bcin13g04870), a gene involved in microtubule interaction and transport (Bcin02g08530), a magnesium transport protein (Bcin04g01090), and a subunit of the fumarate reductase complex (Bcin02g03080). Candidate genes for host specificity include a syntaxin with SNARE domain active in vesicle-mediated transport (Bcin01g01210), a vesicular transport adaptor protein (Clathrin, Bcin11g05660), two major facilitator superfamily (MSF) transporters (Bcin01g01640, Bcin12g01400) and a globin transporting oxygen (Bcin04g06230). The peak at the beginning of chromosome 12 (Fig. 7) is one of two cytochromes P450 (Bcin11g05860, Bcin12g00010) associated with host specificity. Fifty-six out of 131 candidate genes have unknown functions.

Discussion

Generating a matrix of *B. cinerea* disease symptoms across multiple genotypes from eight plant species across four plant orders illustrates the complexity of quantitative host-pathogen interactions. The disease outcome is very different between hosts and cannot be predicted based on phylogenetic distances. Indeed, this study presents *Botrytis cinerea* as a pathogen harboring large phenotypic diversity, sensitive to the resistance mechanisms of its various hosts and with a possible advantage to remain a generalist.

The Genetic Architecture of Botrytis

Many *Botrytis* virulence factors are known such as enzymes contributing to the host tissues breakdown, transporters detoxifying the host defenses and toxicity factors killing the host cells (Nakajima & Akutsu 2013). More than 100 genes have been successfully validated for their effect on the virulence in different

hosts species as documented in the Phi-base database (Urban *et al.* 2016). One of the first functionally validated genes for *B. cinerea* virulence (ten Have *et al.* 1998), the polygalacturonase 1 (Bcin14g00850) active in breakdown of the pectin was identified by GWAS for virulence in agreement with its previously seen selective signatures (Rowe & Kliebenstein 2007). Multiple candidate genes for host specificity and virulence also have the exact or similar functions as functionally validated genes. The redox processes are important for virulence through the production of toxic reactive oxygen species (Viefhues *et al.* 2014). We highlight a subunit of the fumarate reductase respiratory complex and a globin-like ferredoxin as potential candidates active in the redox battle with the host. While the identification of both transmembrane ferroportin and magnesium transporter by GWAS suggest the potential role played by both iron and magnesium, a copper transporter was shown to be essential for the morphology and development of *Botrytis* (Saitoh *et al.* 2010). Finally, an MSF transporter has been shown to contribute to virulence through tolerance of a Brassicaceae phytochemical defense (Vela-Corcia *et al.* 2019) while another ABC transporter was shown to affect the tolerance to the phytoalexin resveratrol and a fungicide (Schoonbeek *et al.* 2001). The quantitative and polygenic architecture of host specificity and virulence can be interpreted as a response to the diverse multi-layer components of plant resistance at large phylogenetic scale. To overcome such diverse resistance, a generalist pathogen might be best equipped by large sets of quantitative genes that through summation of small effect virulence factors can custom the infection to diverse hosts. The absence of phylogenetic signal between host species may be explained by the quantitative and polygenic nature of both resistance and virulence in addition to the interaction of these complex architectures. This interaction is important as it represents alone 16% of the disease outcome.

Botrytis, a jack-of-all-trades pathogen

The *B. cinerea* strains in our collection are generalists that infected all hosts tested in our experimental approach, with only a few strains showing a propensity to prefer an individual host. However, genetic population structures at geographic scale and according to host have been documented in France and Tunisia (Karchani-Balma *et al.* 2008; Mercier *et al.* 2019; Walker *et al.* 2014). *Botrytis* strains obtained from closed environments like intensive greenhouse systems were also shown to display a reduced genetic diversity associated with an increase in clonal distribution (Diao *et al.* 2019; Mercier *et al.* 2019; Walker *et al.* 2014). As such, the environmental condition under which, *B. cinerea* strains specialization might be favored remains unclear as host adaptation, growth facility adaptation or genetic bottlenecks might all also explain genetic patterns observed in *B. cinerea* populations (Calpas *et al.* 2006; Decognet *et al.* 2009; Leyronas *et al.* 2014). The study of the diversity of strain collected from environmental substrates suggest that environmental factors could select for *B. cinerea* strains with rapid mycelial growth and sporulation, increasing the pathogenicity on plants (Bardin 2018). Our experimental approach on plants suggests that generalist strains may have an advantage as they maintain moderate virulence across diverse hosts as specialization may happen by a loss in virulence on most hosts rather than an increase of virulence on a specific host. This model of specialization through loss of virulence is unusual as the inverse pattern; specialization through gain of virulence is the textbook example in pathology (Leggett *et al.* 2013; Woolhouse *et al.* 2001).

Our results are particularly striking in comparison to models explaining host-pathogen qualitative interactions. Qualitative genetic architectures with genes of large-effect tend to co-evolve in the host and the pathogen, following models such as the arms-race scenario (Brown & Tellier 2011; Möller & Stukenbrock 2017). In the arms-race model, defense innovation in the host rapidly selects a novel counter mechanism in the pathogen and virulence is driven by evolution in large effect genes linked to this interaction. This co-evolution leads to a model in which specialized strains arise from a population of weakly virulent generalists, with a strong directional pressure in pathogens to become specialists (Barrett *et al.* 2009; Leggett *et al.* 2013; Woolhouse *et al.* 2001). Other qualitative models than the arm-races model such as the inversed gene-for-gene, matching alleles or inversed matching alleles models (Morris & Moury 2019) don't fit *B. cinerea* well either.

The challenge of mapping quantitative interactions

The host-pathogen quantitative interactions may be best explained by an additive model. In such a model,

the elements of the quantitative architectures are gene networks that cooperate or interfere with each other within species but also across interacting species. Other factors such as epistasis might also impact such gene networks and their interactions. The cross-kingdom genetic interactions have been shown through cross-kingdom gene expression networks (Zhang *et al.* 2019), the existence of loci in the pathogen genome controlling gene expression of both host and pathogen (Soltis *et al.* 2020) and also through RNA interference (Weiberg *et al.* 2013). To understand quantitative interactions, large-scale genomic studies are needed to reveal how conserved and predictable are those networks interactions. The modeling of such complex interactions will be beneficial not only to understand host-pathogen interactions such as generalist pathogens but also more largely for ecological interactions. Although ecological interactions are beginning to be understood through the glass of large effect genes with community effects, quantitative genetic architectures hide behind it. The modeling of quantitative-only systems such as the *Botrytis* pathosystem will provide a framework to understand the small effect architectures behind ecological interactions at large.

Acknowledgments: Seeds used in this study were provided by Laura Marek and Kathleen Reitsma at the US department of agriculture, Chris Pires, the UC Davis Tomato Genetics Resource Center, the Center for Genetic Resources Netherland (CGN) through Guy Barker and Graham Teakle. The experiments were performed with the help of Dihan Gao, Aysha Shafi, David Kelly, Matisse Madrone, Melissa Wang, Josue Vega, Aleshia Hopper and Ayesha Siddiqui. **Funding:** NSF IOS 1339125 and 1021861 to DJK.

Data Accessibility:

Correspondence and requests for materials should be addressed to Kliebenstein@ucdavis.edu. R codes and datasets are available on github.com/CaseysC/Eudicot.Rcode. The whole genome SNP data for 95 *Botrytis cinerea* strains used for GWAS is available on Dryad <https://doi.org/10.25338/B83P56>.

Author contributions:

Conceptualization and supervision: DJK; Data analysis: CC; Founding acquisition: DJK, Investigation: GS, CC, NS, RG, JC; Resources: SA; Writing: CC, DJK. The authors declare no competing interests.

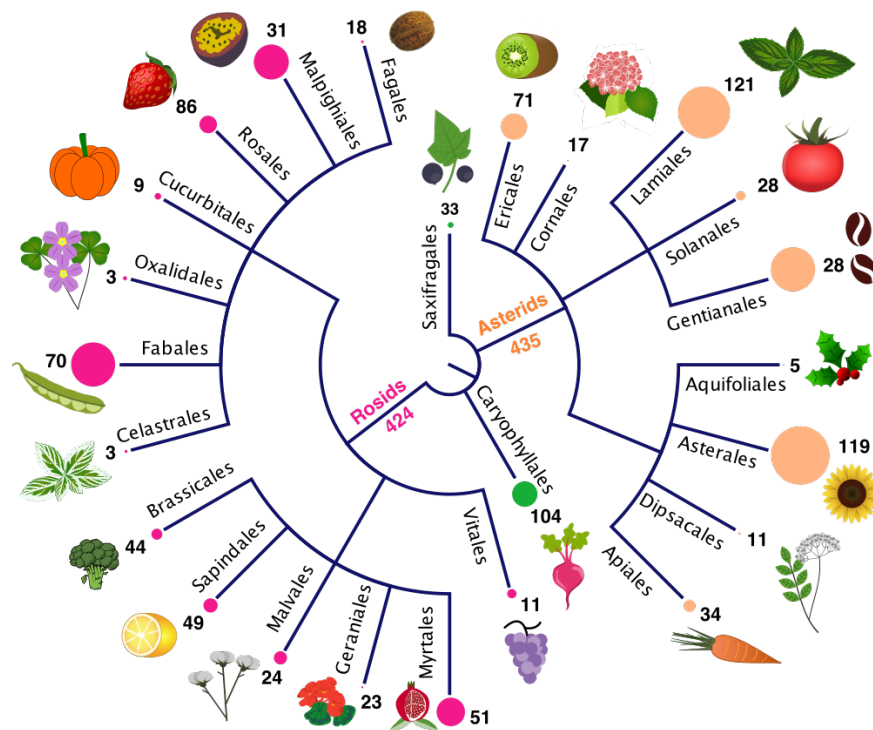


Fig. 1: Disease symptoms caused by *Botrytis cinerea* observed on plants from the core Eudicots. The list of plant species with disease symptoms were extracted from Elad et al. (2016). The tree represents major orders from the basal Eudicots (in green), Asterids (in orange) and Rosids (in pink). The size of the circle at the end of the branches is proportional to the species diversity of the order. The species diversity was extracted from the Missouri Botanical garden angiosperm phylogeny (<http://www.mobot.org/MOBOT/Research/APweb/>). For each order, the number of species with known disease symptom is indicated.

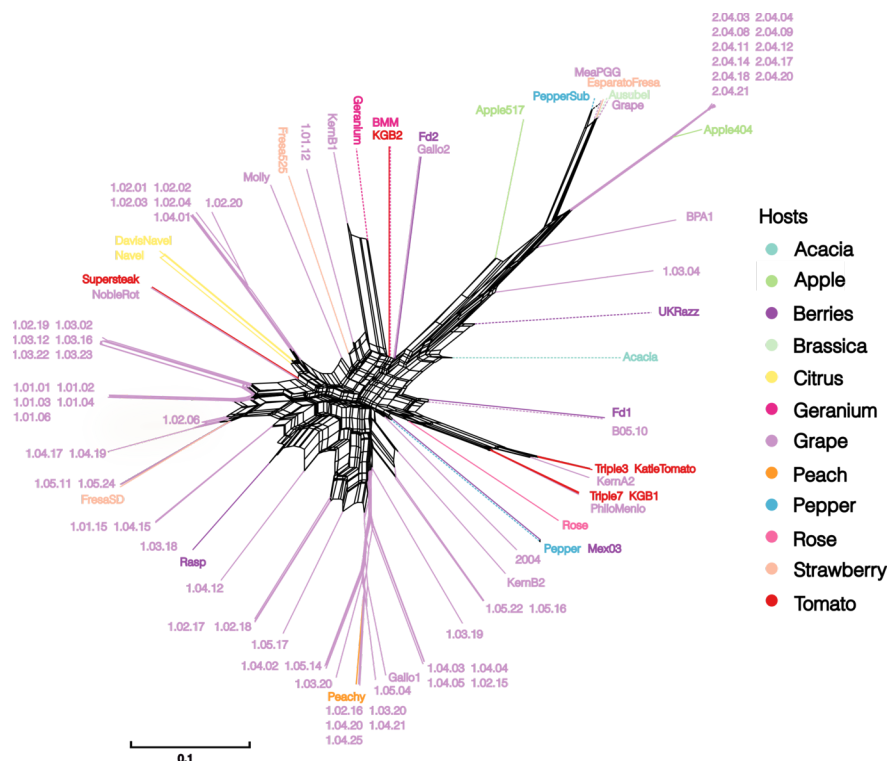


Fig 2: Population structure and genetic distances in the *Botrytis* strain collection. Color represent the host the strains were collected from. Dashed lines represent strains collected outside of California.

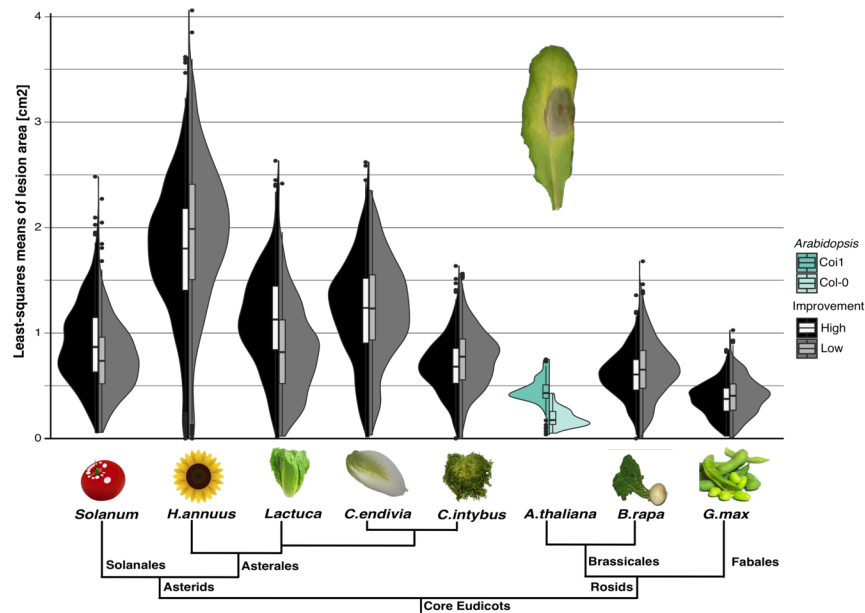


Fig. 3: Lesion areas at 72 hours post inoculation on seven crop species shows small and inconsistent effect of domestication on the *Botrytis cinerea* interaction . Half-violins and boxplots (median and interquartile range) represent the mean lesion area distribution of high (black, n=588) and low (grey, n=588) improvement genotypes for all 98 *Botrytis* strains. *Lactuca* refers to *Lactuca sativa* for high and *Lactuca serriola* for low improvement genotypes. *Solanum* refers to *Solanum lycopersicum* for high and *Solanum pimpinellifolium* for low improvement genotypes. As reference, virulence on *A. thaliana* wild-type (Col-0, n=98) and jasmonic acid signaling mutant (*coi1*, n=98) are presented. The non-scaled tree represents the phylogenetic relationship between eudicot species. A lesion example on an *A. thaliana* leaf is provided.

Hosted file

image4.emf available at <https://authorea.com/users/375680/articles/492845-modeling-quantitative-interactions-the-disease-outcome-of-generalist-fungal-pathogen-across-the-plant-kingdom>

New Fig. 4: Host variation predominates the outcomes of plant-*Botrytis* interactions across species while *Botrytis* variation predominates within plant species. A) Multi-host linear model estimating the contribution of plant species, plant genotypes, improvement status, *Botrytis* strains and their interaction on the percentage of variance in lesion area. B) Species-specific linear mixed models that estimate the percentage of variance in lesion area. In grey are the experimental parameters classed as random factors. Two-tailed t-test: *p<0.05, **p<0.01, ***p<0.005.

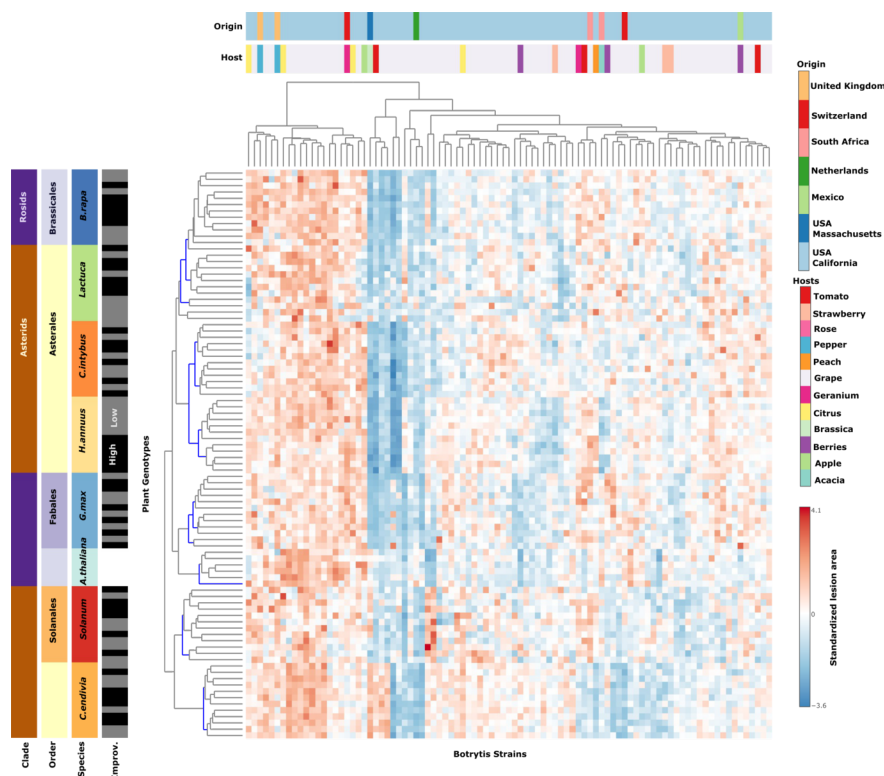


Fig.5: Variation of plant susceptibility in the Botrytis pathosystem is species specific and does not track plant evolution. Heatmap of standardized (z-scored) least-squares means of lesion area (n=6) for Botrytis strains (x-axis) interacting with 90 plant genotypes (y-axis). The strains were isolated largely in California (light blue color in the origin bar) and on grape (light purple in the host bar). For *A. thaliana*, five single gene knockout mutants and the corresponding wild-type Col-0 are presented. For the seven crop species, six genotypes with low (grey) and high (black) improvement are presented. The seven crop species were chosen to represent a wide spectrum of phylogenetic distances across Rosids (Brassicales and Fabales) and Asterids (Asterales and Solanales). Branches in the dendrogram that are supported with 95% certainty after bootstrapping are indicated in blue. No branches in the Botrytis strain dendrogram were significant.

Hosted file

image6.emf available at <https://authorea.com/users/375680/articles/492845-modeling-quantitative-interactions-the-disease-outcome-of-generalist-fungal-pathogen-across-the-plant-kingdom>

Fig. 6: Strains with low virulence have high host specificity. A) Estimates of virulence (average lesion area) and host specificity (coefficient of variation) across eight eudicots for the Botrytis strains are shown. The strains are colored according to the plant host from which they were collected. A quadratic relationship was the optimal description of the relationships between specificity and virulence and is shown with a grey confidence interval ($R^2=0.44$, $P=6.36 \times 10^{-13}$). B) Mean lesion area and standard error (n=12, except *A. thaliana* n=6) across the eight eudicot species is provided for two strains at the extremes of the host specificity/virulence distribution.

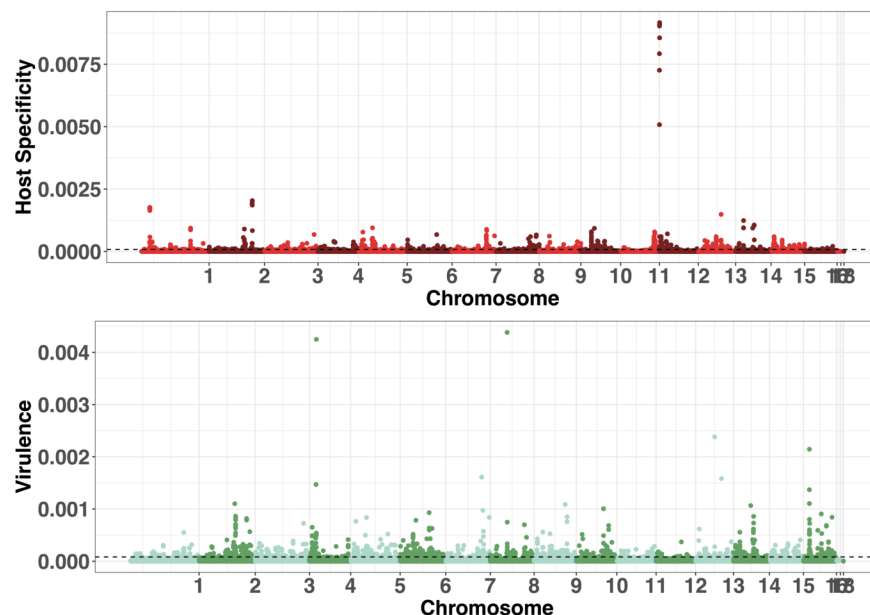


Fig. 7: Botrytis virulence and host specificity genetic architecture is polygenic. GWAS significance of 271,749 SNPs estimated as posterior inclusion probability (PIP) of Bayesian sparse linear mixed model for host specificity (in red) and virulence (in green). The dashed lines represent a probability of false positive $p < 0.01$ based on the tail of the PIP distribution of 20 random permutation tests.

Hosted file

image8.emf available at <https://authorea.com/users/375680/articles/492845-modeling-quantitative-interactions-the-disease-outcome-of-generalist-fungal-pathogen-across-the-plant-kingdom>

Fig. S1: Experimental Design. We tested the virulence of 98 *Botrytis cinerea* strains on seven eudicot crop species and the plant model *A.thaliana* using randomized complete block design detached leaf assays with 6-fold replication.

Hosted file

image9.emf available at <https://authorea.com/users/375680/articles/492845-modeling-quantitative-interactions-the-disease-outcome-of-generalist-fungal-pathogen-across-the-plant-kingdom>

Fig. S2: Geographical origin of the 84 Eudicot genotypes selected for this study. *B. rapa* samples come from all over the world, *C. endivia*, *C. intybus*, *Lactuca* and *G. max* come from Eurasia, *H. annuus* come from North America and *Solanum* from South America. Colored symbols represent the species and improvement status.

Hosted file

image10.emf available at <https://authorea.com/users/375680/articles/492845-modeling-quantitative-interactions-the-disease-outcome-of-generalist-fungal-pathogen-across-the-plant-kingdom>

New Fig. S3: Variance in lesion area in *Arabidopsis thaliana*. A) Violin and boxplot represent the mean lesion area distribution for genotypes affecting camalexin synthesis (red), jasmonic acid signaling (green), salicylic acid signaling (blue) in comparison to the wild-type Col0 (purple) for all 98 *Botrytis* strains. B) Species-specific linear mixed model that estimate the percentage of variance in lesion area. In grey are the experimental parameters used as random factor. Two-tailed t-test: * $p < 0.05$, ** $p < 0.01$, *** $p < 0.005$.

Fig. S4: Modeling of host specificity based on mean lesion area for the 98 Botrytis strains.

A) Comparison of the standardized lesion area of the preferred host (largest lesion) to the mean of the seven remaining species. The 1:1 line represent a theoretical ‘generalism’ in which strains would infect all host with equal virulence. The grey area is mathematically impossible. B) The quadratic relation between standardized mean lesion area on the remaining seven hosts and the distance to generalism confirm the trend of Figure 5, without considering the variance in lesion area.

Hosted file

image13.emf available at <https://authorea.com/users/375680/articles/492845-modeling-quantitative-interactions-the-disease-outcome-of-generalist-fungal-pathogen-across-the-plant-kingdom>

Figure S5: Sliding-Window analysis of effect size along the chromosomes for host specificity (coefficient of variation of lesion area) and virulence (mean lesion area). The GWAS methods are linear model in Gemma (LM), Ridge regression in BigRR (RR) and Bayesian sparse linear mixed model in Gemma (BSLMM).

Supplementary Tables :

Table S1: Information for 84 accessions of seven crop species. The accession ID corresponds to the germplasm collections (the U.S. Department of Agriculture Germplasm Resources Information Network [USDA Grin], the Centre for Genetic resources in the Netherland [CGN], UC Davis Tomato Genetic Resource Center [TGRC]). Information on the species and subspecies, Taxon, order, clade, improvement status, cultivar name, geographical origin in addition to latitude and longitude coordinates are provided when available.

Table S2: Germination and growth conditions for the eight eudicot species . All plants were grown in growth chambers at 20°C with 16h hours photoperiod at 100-120 mE light intensity for four to eight weeks to account for the different developmental rates.

Table S3: Information for the 98 strains of *Botrytis cinerea* . The name of the isolates, geographical origin with latitude and longitude coordinates (when available), the name and affiliation of the person who collected the strain, the year of isolation and plant species (host) on which the strain was collected are provided.

Table S4: Maximum lesion size and median thresholds. These thresholds were used for the partitioning of technical and biological failures in developing lesions as well as the percentage of data points removed in each of the eight eudicot species.

Table S5: Detailed results for the nine linear and mixed models performed in this study, plotted in Fig. 3 and Fig. S4. For each model, the R formula and syntax are provided. For each model and factor, the statistics (chi or sum of square), percent of variance, degree of freedom and p-values are provided.

Table S6: Percentage of significant SNPs detected by the GWAS of the virulence (Vir) and host specificity (Spe) relative to the total number of SNPs per chromosomes or genetic regions. The GWAS methods are linear model in Gemma (LM), Ridge regression in BigRR (RR) and bayesian sparse linear mixed model in Gemma (BSLMM).

Table S7: Information on the 131 genes with functional effect SNPs identified by GWAS for virulence and host specificity. Location in the B05.10 reference genome and various functional annotations are provided.

References

- Atwell S, Corwin J, Soltis N, *et al.* (2018) Resequencing and association mapping of the generalist pathogen *Botrytis cinerea*. *bioRxiv* , 489799.
- Atwell S, Corwin JA, Soltis NE, *et al.* (2015) Whole genome resequencing of *Botrytis cinerea* isolates identifies high levels of standing diversity. *Frontiers in Microbiology* **6** , 987.
- Bardin M (2018) Striking Similarities Between *Botrytis cinerea* From Non-agricultural and From Agricultural Habitats. In: *fpls-09-01820.tex* , pp. 1-11.
- Barrett LG, Kniskern JM, Bodenhausen N, Zhang W, Bergelson J (2009) Continua of specificity and virulence in plant host-pathogen interactions: causes and consequences. In: *The New phytologist* , pp. 513-529.
- Berens ML, Berry HM, Mine A, Argueso CT, Tsuda K (2017) Evolution of Hormone Signaling Networks in Plant Defense. In: *Annu Rev Phytopathol* , pp. 401-425.
- Bertazzoni S, Williams AH, Jones DA, *et al.* (2018) Accessories Make the Outfit: Accessory Chromosomes and Other Dispensable DNA Regions in Plant-Pathogenic Fungi. In: *Molecular plant-microbe interactions : MPMI* , pp. 779-788.
- Bialas A, Zess EK, De la Concepcion JC, *et al.* (2018) Lessons in Effector and NLR Biology of Plant-Microbe Systems. In: *Molecular plant-microbe interactions : MPMI* , pp. 34-45.
- Bird KA, An H, Gazave E, *et al.* (2017) Population structure and phylogenetic relationships in a diverse panel of *Brassica rapa* L. *Frontiers in plant science* **8** , 321.
- Brown JKM, Tellier A (2011) Plant-Parasite Coevolution: Bridging the Gap between Genetics and Ecology. In: *Annu Rev Phytopathol* , pp. 345-367.
- Calpas JT, Korschuh MN, Toews CC, Tewari JP (2006) Relationships among isolates of *Botrytis cinerea* collected from greenhouses and field locations in Alberta, based on RAPD analysis. *Can. J. Plant Pathol* , 1-16.

- Chae L, Kim T, Nilo-Poyanco R, Rhee SY (2014) Genomic Signatures of Specialized Metabolism in Plants. In: *Science* , pp. 510-513.
- Chen YH, Gols R, Benrey B (2015) Crop domestication and its impact on naturally selected trophic interactions. *Annual Review of Entomology* **60** , 35-58.
- Cingolani P, Platts A, Wang LL, *et al.* (2012) A program for annotating and predicting the effects of single nucleotide polymorphisms, SnpEff: SNPs in the genome of *Drosophila melanogaster* strain w1118; iso-2; iso-3. *Fly* **6** , 80-92.
- Corwin JA, Copeland D, Feusier J, *et al.* (2016) The Quantitative Basis of the Arabidopsis Innate Immune System to Endemic Pathogens Depends on Pathogen Genetics. In: *PLoS Genet* , p. e1005789.
- Corwin JA, Kliebenstein DJ (2017) Quantitative Resistance: More Than Just Perception of a Pathogen. In: *The Plant Cell Online* , pp. 655-665.
- Cosseboom SD, Ivors KL, Schnabel G, Bryson PK, Holmes GJ (2019) Within-Season Shift in Fungicide Resistance Profiles of *Botrytis cinerea* in California Strawberry Fields. *Plant Dis* **103** , 59-64.
- Cowger C, Brown JKM (2019) Durability of Quantitative Resistance in Crops: Greater Than We Know? In: *Annu Rev Phytopathol* , pp. 253-277.
- De Gracia M, Cascales M, Expert P, *et al.* (2015) How Did Host Domestication Modify Life History Traits of Its Pathogens? In: *PLoS One* , p. e0122909.
- De Vries I (1997) Origin and domestication of *Lactuca sativa* L. *Genetic Resources and Crop Evolution* **44** , 165-174.
- Decognet V, Bardin M, Trottin-Caudal Y, Nicot P (2009) Rapid change in the genetic diversity of *Botrytis cinerea* populations after the introduction of strains in a tomato glasshouse. *Phytopathology* **99** , 185-193.
- Delplace F, Huard-Chauveau C, Dubiella U, *et al.* (2020) Robustness of plant quantitative disease resistance is provided by a decentralized immune network. In: *Proceedings of the National Academy of Sciences* , pp. 18099-18109.
- Dempewolf H, Rieseberg LH, Cronk QC (2008) Crop domestication in the Compositae: a family-wide trait assessment. *Genetic Resources and Crop Evolution* **55** , 1141-1157.
- Denby KJ, Kumar P, Kliebenstein DJ (2004) Identification of *Botrytis cinerea* susceptibility loci in *Arabidopsis thaliana*. In: *Plant J* , pp. 473-486.
- Diao Y, Larsen M, Kamvar ZN, *et al.* (2019) Genetic differentiation and clonal expansion of Chinese *Botrytis cinerea* populations from tomato and other crops in China. *Phytopathology* .
- Dong S, Raffaele S, Kamoun S (2015) The two-speed genomes of filamentous pathogens: waltz with plants. In: *Curr Opin Genet Dev* , pp. 57-65. Elsevier Ltd.
- Elad Y, Pertot I, Cotes Prado AM, Stewart A (2016) Plant Hosts of *Botrytis* spp. In: *Botrytis – the Fungus, the Pathogen and its Management in Agricultural Systems* (eds. Fillinger S, Elad Y), pp. 413-486. Springer International Publishing, Cham.
- Fillinger S, Elad Y (2015) *Botrytis – the Fungus, the Pathogen and its Management in Agricultural Systems* Springer.
- Fordyce RF, Soltis NE, Caseys C, *et al.* (2018) Digital Imaging Combined with Genome-Wide Association Mapping Links Loci to Plant-Pathogen Interaction Traits. In: *PLANT PHYSIOLOGY* , pp. 1406-1422.
- Frantzeskakis L, Di Pietro A, Rep M, *et al.* (2020) Rapid evolution in plant-microbe interactions – a molecular genomics perspective. In: *The New phytologist* , pp. 1134-1142.

- Glazebrook J (2005) Contrasting mechanisms of defense against biotrophic and necrotrophic pathogens. *Annu. Rev. Phytopathol.* **43** , 205-227.
- Glazebrook J, Roby D (2018) Plant biotic interactions: from conflict to collaboration. In: *Plant J* , pp. 589-591.
- Goudet J (2005) Hierfstat, a package for R to compute and test hierarchical F-statistics. *Molecular Ecology Notes* **5** , 184-186.
- Herman M, Williams M (2012) Fighting for their lives: Plants and pathogens. *The Plant Cell* **24** , tpc.112.tt0612.
- Huson DH, Bryant D (2006) Application of phylogenetic networks in evolutionary studies. *Molecular Biology And Evolution* **23** , 254-267.
- Inupakutika MA, Sengupta S, Devireddy AR, Azad RK, Mittler R (2016) The evolution of reactive oxygen species metabolism. In: *Journal of Experimental Botany* , pp. 5933-5943.
- Jacob F, Vernaldi S, Maekawa T (2013) Evolution and conservation of plant NLR functions. *Frontiers in immunology* **4** , 297.
- Karasov TL, Horton MW, Bergelson J (2014) Genomic variability as a driver of plant–pathogen coevolution? In: *Curr Opin Plant Biol* , pp. 24-30. Elsevier Ltd.
- Karchani-Balma S, Gautier A, Raies A, FOURNIER E (2008) Geography, Plants, and Growing Systems Shape the Genetic Structure of Tunisian Botrytis cinerea Populations. In: *Phytopathology* , pp. 1271-1279.
- Krah F-S, Bässler C, Heibl C, *et al.* (2018) Evolutionary dynamics of host specialization in wood-decay fungi. *BMC Evolutionary Biology* **18** , 119.
- Lannou C (2012) Variation and selection of quantitative traits in plant pathogens. *Annual review of phytopathology* **50** , 319-338.
- Leggett HC, Buckling A, Long GH, Boots M (2013) Generalism and the evolution of parasite virulence. In: *Trends Ecol Evol* , pp. 592-596. Elsevier Ltd.
- Lenth R, Singmann H, Love J, Buerkner P, Herve M (2018) Emmeans: Estimated marginal means, aka least-squares means. *R package version* **1** , 3.
- Leyronas C, Bardin M, Duffaud M, Nicot PC (2015) Compared dynamics of Grey Mould incidence and genetic characteristics of Botrytis cinerea in neighbouring vegetable greenhouses. *Journal of plant pathology* **97** , 439-447.
- Leyronas C, Bryone F, Duffaud M, Troulet C, Nicot PC (2014) Assessing host specialization of Botrytis cinerea on lettuce and tomato by genotypic and phenotypic characterization. In: *Plant Pathology* , pp. 119-127.
- Li M-X, Yeung JMY, Cherny SS, Sham PC (2012) Evaluating the effective numbers of independent tests and significant p-value thresholds in commercial genotyping arrays and public imputation reference datasets. *Human Genetics* **131** , 747-756.
- Lin T, Zhu G, Zhang J, *et al.* (2014) Genomic analyses provide insights into the history of tomato breeding. *Nature genetics* **46** , 1220-1226.
- Lischer HEL, Excoffier L (2011) PGDSpider: an automated data conversion tool for connecting population genetics and genomics programs. *Bioinformatics* **28** , 298-299.
- Ma Z, Michailides TJ (2005) Genetic Structure of Botrytis cinerea Populations from Different Host Plants in California. *Plant Disease* **89** , 1083-1089.

- Mercier A, Carpentier F, Duplaix C, *et al.* (2019) The Polyphagous plant pathogenic fungus *Botrytis cinerea* encompasses host-specialized and generalist populations. In: *bioRxiv* , pp. 1-25.
- Meyer RS, DuVal AE, Jensen HR (2012) Patterns and processes in crop domestication: an historical review and quantitative analysis of 203 global food crops. *New Phytologist* **196** , 29-48.
- Möller M, Stukenbrock EH (2017) Evolution and genome architecture in fungal plant pathogens. In: *Nature Publishing Group* , pp. 1-16. Nature Publishing Group.
- Morris CE, Moury B (2019) Revisiting the Concept of Host Range of Plant Pathogens. In: *Annu Rev Phytopathol* , pp. 63-90.
- Mou B (2011) Mutations in lettuce improvement. *International Journal of Plant Genomics* **2011** .
- Nakajima M, Akutsu K (2013) Virulence factors of *Botrytis cinerea*. *Journal of General Plant Pathology* **80** , 15-23.
- Plissonneau C, Benevenuto J, Mohd-Assaad N, *et al.* (2017) Using Population and Comparative Genomics to Understand the Genetic Basis of Effector-Driven Fungal Pathogen Evolution. In: *Frontiers in plant science* , p. 656.
- Poisot T, Canard E, Mouquet N, Hochberg ME (2012) A comparative study of ecological specialization estimators. *Methods in Ecology and Evolution* **3** , 537-544.
- Poland JA, Balint-Kurti PJ, Wisser RJ, Pratt RC, Nelson RJ (2009) Shades of gray: the world of quantitative disease resistance. In: *Trends Plant Sci* , pp. 21-29.
- Rowe HC, Kliebenstein DJ (2007) Elevated genetic variation within virulence-associated *Botrytis cinerea* polygalacturonase loci. *Molecular Plant-Microbe*
- Rowe HC, Walley JW, Corwin JA, *et al.* (2010) Deficiencies in Jasmonate-Mediated Plant Defense Reveal Quantitative Variation in *Botrytis cinerea* Pathogenesis. *PLoS Pathogens* **6** , e1000861.
- Saito S, Xiao CL (2018) Fungicide Resistance in *Botrytis cinerea* Populations in California and its Influence on Control of Gray Mold on Stored Mandarin Fruit. *Plant Dis* **102** , 2545-2549.
- Saitoh Y, Izumitsu K, Morita A, Tanaka C (2010) A copper-transporting ATPase BcCCC2 is necessary for pathogenicity of *Botrytis cinerea*. In: *Mol Genet Genomics* , pp. 33-43.
- Schep AN, Kummerfeld SK (2017) iheatmapr: interactive complex heatmaps in R. *Journal of Open Source Software* **2** , 359.
- Schoonbeek H, Del Sorbo G, De Waard M (2001) The ABC transporter BcatrB affects the sensitivity of *Botrytis cinerea* to the phytoalexin resveratrol and the fungicide fenpiclonil. *Molecular plant-microbe interactions* **14** , 562-571.
- Shen X, Alam M, Fikse F, Rönnegård L (2013) A novel generalized ridge regression method for quantitative genetics. *Genetics* **193** , 1255-1268.
- Soltis NE, Atwell S, Shi G, *et al.* (2019) Crop domestication and pathogen virulence: Interactions of tomato and *Botrytis* genetic diversity. *The Plant Cell* **31** , 502-519.
- Soltis NE, Caseys C, Zhang W, *et al.* (2020) Pathogen genetic control of transcriptome variation in the Arabidopsis thaliana–*Botrytis cinerea* pathosystem. *Genetics* **215** , 253-266.
- Sørensen I, Domozych D, Willats WG (2010) How have plant cell walls evolved? *PLANT PHYSIOLOGY* **153** , 366-372.
- Suzuki R, Shimodaira H (2006) Pvcust: an R package for assessing the uncertainty in hierarchical clustering. *Bioinformatics* **22** , 1540-1542.

- ten Have A, Mulder W, Visser J, van Kan JAL (1998) The endopolygalacturonase gene Bcpg1 is required for full virulence of *Botrytis cinerea*. In: *Molecular plant-microbe interactions : MPMI* , pp. 1009-1016.
- Upton JL, Zess EK, Bialas A, Wu C-H, Kamoun S (2018) The coming of age of EvoMPMI: evolutionary molecular plant-microbe interactions across multiple timescales. In: *Curr Opin Plant Biol* , pp. 108-116. Elsevier Ltd.
- Urban M, Cuzick A, Rutherford K, *et al.* (2016) PHI-base: a new interface and further additions for the multi-species pathogen-host interactions database. *Nucleic acids research* **45** , D604-D610.
- van der Does HC, Rep M (2007) Virulence genes and the evolution of host specificity in plant-pathogenic fungi. In: *Molecular plant-microbe interactions : MPMI* , pp. 1175-1182.
- Van Kan JA, Stassen JH, Mosbach A, *et al.* (2017) A gapless genome sequence of the fungus *Botrytis cinerea*. *Molecular plant pathology* **18** , 75-89.
- Vela-Corcia D, Aditya Srivastava D, Dafa-Berger A, *et al.* (2019) MFS transporter from *Botrytis cinerea* provides tolerance to glucosinolate-breakdown products and is required for pathogenicity. *Nat Commun* **10** , 2886.
- Veloso J, van Kan JAL (2018) Many Shades of Grey in Botrytis-Host Plant Interactions. *Trends in plant science* **23** , 613-622.
- Vieffhues A, Heller J, Temme N, Tudzynski P (2014) Redox Systems in *Botrytis cinerea*: Impact on Development and Virulence. In: *Mol Plant Microbe In* , pp. 858-874.
- Walker A-S, Gladieux P, Decognet V, *et al.* (2014) Population structure and temporal maintenance of the multihost fungal pathogen *Botrytis cinerea*: causes and implications for disease management. *Environmental Microbiology* **17** , 1261-1274.
- Walley PG, Hough G, Moore JD, *et al.* (2017) Towards new sources of resistance to the currant-lettuce aphid (*Nasonovia ribisnigri*). *Molecular Breeding* **37** , 4.
- Weiberg A, Wang M, Lin F-M, *et al.* (2013) Fungal small RNAs suppress plant immunity by hijacking host RNA interference pathways. *Science* **342** , 118-123.
- Weir BS, Cockerham CC (1984) Estimating F-statistics for the analysis of population structure. *Evolution* , 1358-1370.
- Whitehead SR, Turcotte MM, Poveda K (2017) Domestication impacts on plant-herbivore interactions: a meta-analysis. *Philosophical Transactions of the Royal Society B: Biological Sciences* **372** , 20160034.
- Wilkinson SW, Magerøy MH, Sánchez AL, *et al.* (2019) Surviving in a Hostile World: Plant Strategies to Resist Pests and Diseases. *Annual review of phytopathology* **57** , 505-529.
- Woolhouse ME, Taylor LH, Haydon DT (2001) Population biology of multihost pathogens. *Science* **292** , 1109-1112.
- Zhang W, Corwin JA, Copeland D, *et al.* (2017) Plastic Transcriptomes Stabilize Immunity to Pathogen Diversity: The Jasmonic Acid and Salicylic Acid Networks within the Arabidopsis/ *Botrytis* Pathosystem. In: *The Plant Cell Online* , pp. 2727-2752.
- Zhang W, Corwin JA, Copeland DH, *et al.* (2019) Plant-necrotroph co-transcriptome networks illuminate a metabolic battlefield. In: *eLife* .
- Zhou X, Carbonetto P, Stephens M (2013) Polygenic modeling with Bayesian sparse linear mixed models. *PLoS Genet* **9** , e1003264.